Influence of Iodine Doping on the Structural and Electronic Properties of $CsSnBr_3$

DILSHOD NEMATOV [1,2,*]

[1] S.U.Umarov Physical -Technical Institute of National Academy of Sciences of Tajikistan
[2] M.S.Osimi Tajik Technical University, Dushanbe, 724000 TAJIKISTAN

Abstract: In this work, by means of quantum-chemical calculations within the framework of density functional theory, the considered several structural and electronic properties of nanocrystals of the CsSnBr3−xIx (0≤x≤3) and discussed the effect of iodine concentration on the geometry and electronic properties of these materials. The exchange-correlation effects of electrons were taken into account by the LDA, GGA, and the modified Becke-Jones exchange-correlation potential (mBJ). The results obtained in the framework of the DFT-mBJ and the Wien2k package are in good agreement with the data from experimental measurements and open up the possibility of accurately predicting a number of fundamental properties of perovskite-like complex structures and the development of new materials.

Keywords: density functional theory; band gap; electronic structure; perovskite; Wien2k package.
Received: June 19, 2021. Revised: April 26, 2022. Accepted: June 15, 2022. Published: July 29, 2022.

1. Introduction

The possibilities of converting solar energy and other unconventional forms of energy into electricity are considered in the context of projected global energy needs for the 21st century [1-3]. Therefore, a very urgent task facing scientists and engineers today is the study of several electronic, optical, thermal, and other characteristics of new materials with the aim of their application in solar energy. Furthermore, to successfully transition from fossil fuels to renewable energies, confront climate change, and end pollution, we can no longer rely solely on existing materials but must focus on synthesizing other classes of materials with improved properties. Moreover, the energy demand constantly increases with population growth, and the gap between demand and supply also widens over time [1-3].

Conventional energy production methods will no longer be able to meet the world's energy needs. Therefore, unconventional measures, including the creation of photovoltaic devices, wind farms, and moisture-to-electricity converters, are of great interest, and for the implementation of these tasks and the transition to Green Energy, countries of the world allocate a huge amount of money and support scientists and engineers to strengthen their research works [1].

The effect of converting light into electricity was discovered back in 1839 by Alexander Edmond Becquerel, after which Charles Frits and Jacamo Luigi made the first attempt to create the first light-to-electricity converter. However, this unique discovery did not attract the attention of researchers due to the then low coefficient transformation. Over the years, attempts have been made to increase the photoelectric conversion factor of solar cells, which were created on the basis of silicon, gallium arsenide, and other semiconductor materials. As a tradition for creating solar cells, silicon composites have been widely used due to their unique electrophysical properties, such as bandgap and light absorption capacity. However, at the moment, the maximum conversion efficiency of commercially available silicon converters is only 14-15% [2]. Moreover, the technology for the production of traditional silicon-based solar cells is advanced, but some problems such as high cost and environmental pollution need to be addressed.

In 2013, Science magazine reported on the possibility of using perovskites in solar cells [3]. According to the National Laboratory for Renewable Energy Sources (NREL), perovskites are also widely used in memory devices, LEDs, diodes for ultra-high-power lasers, etc. [4], due to their low cost, high

absorption coefficient, high mobility of charge carriers, composite flexibility, high stability, and adjustable material structure. The only natural perovskite, calcium titanate ($CaTiO_3$), was discovered by Gustav Rose in 1839 and was named perovskite in honor of Count L.A. Perovsky. Later, the artificial synthesis of these structures began with the general formula ABX_3, where X = F^-, Cl^-, Br^-, I^-, and O^{2-}. Elements A and B are two cations of different sizes.

Features and prospects of the use of halide-based perovskites are that it can be tuned either by changing the content of halides or by using the size of the cations to obtain the optimal bandgap for photovoltaic applications. Moreover, the efficiency of perovskite panels is practically already exceeded by 26.7% [5]. However, despite the rapid progress made over the past few years in terms of conversion efficiency, understanding the fundamental properties of perovskites is rather limited. Proceeding from this, the aim of this work is a quantum-chemical study of the geometric and electronic properties of I-doped perovskite nanostructures based on $CsSnBr_3$ in order to find the regularity of the change in their properties under the influence of iodine concentration, as well as to reveal the expediency of further experimental study of the properties of these nanocrystals.

2. Materials and Methods

Ab initio quantum-chemical calculations within the framework of the density functional theory [6] were implemented in the Wien2k package [7]. The DFT is a method based on *ab initio* calculation initially proposed by Hohenberg [8], Kohn, and Sham [9], which has the advantage of not relying on any experimental parameter. The idea of this method is to replace the interacting electronic system by a fictitious non-interacting electronic system that gives the same electronic density as the interacting system. The XC potential affecting the non-interacting electronic system can be obtained from the XC energy, which is only a function of the electronic density. However, no exact functional exists, but many approximative functionals have been developed, for example, LDA, GGA. The object under study was the orthorhombic structures of nanocrystals of the $CsSnBr_{3-x}I_x$ ($0 \le x \le 3$) family (systems $CsSnBr_3$, $CsSnBr_2I$, $CsSnBrI_2$ и $CsSnI_3$). The radius of the Mufftin sphere (RMT) for Cs, Sn, and I was taken as $2.5a_0$, and for Br - $2.07a_0$, where a_0 is the Bohr radius. Nevertheless, the crystal structures of the materials under study are shown in Figure 1.

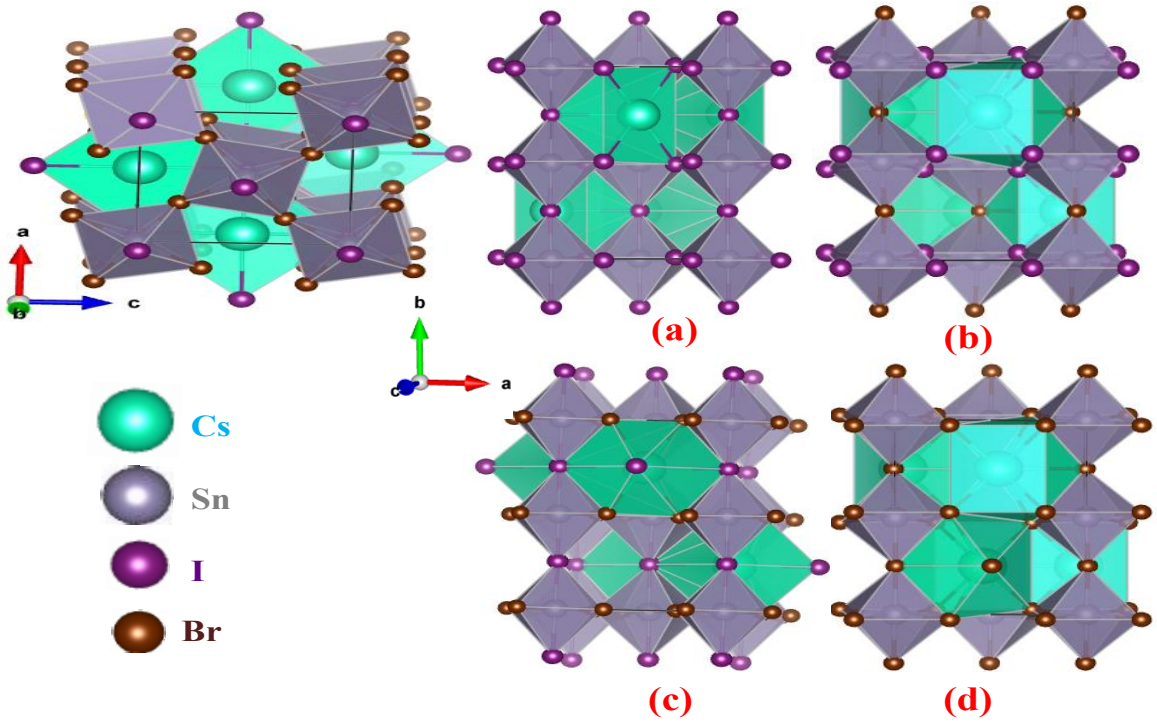

Figure 1. Schematic illustration of crystal structures of **(a)** $CsSnBr_3$, **(b)** $CsSnBr_2I$, **(c)** $CsSnBrI_2$ and **(d)** $CsSnI_3$.

The valence wave functions inside the MT sphere were expanded to lmax = 10, and the charge density was expanded in a Fourier series up to Gmax. For sufficiently good convergence in the parameters of the total crystal lattice energy, all atomic geometry optimizations for the orthorhombic unit cell of $CsSnBr_{3-x}I_x$ system were performed using k-points generated by uniform grid parameters 3 × 2 × 3.

In addition to using the LDA and GGA approximations, the study of electronic properties required the use of the modified Becke-Johnson potential (TB-mBJ) [10], the formulation of which is given as follows:

$$E_{xc}^{mBJ}(r) = cE_x^{BR}(r) + (3c-2)\frac{1}{\pi}\sqrt{\frac{5k(r)}{6\rho(r)}} \quad (1),$$

where k (r) is the kinetic energy density according to the Kohn - Sham equation, is the spin-dependent electron density, and E_x^{BR} - is the Becke - Roussel exchange functional (BR). c, is the added parameter by Tran and Blaha to the mBJ potential.

TB-mBJGGA and TBmBJ + LDA potentials, whose mBJ exchange potential is available in the LIBXC interface library [11], are used in combination with lattice parameters optimized by the GGA and LDA approximations.

c), volume (V), and angles between a, b and c) is inevitable for describing the structural properties of materials. The equilibrium lattice parameters of the materials under study are determined after optimization, where all these materials have the space group Pnma (62). Equilibrium lattice parameters were obtained by approximating the total energy as a function of the normalized volume, according to the equation of state of the ground state (EOS), the analytical expression of which is determined using the Birch-Murnaghan approximation [12]:

$$E(V) = E_0 + \frac{9}{8}B_0V_0\left[\left(\frac{V_0}{V}\right)^{2/3}-1\right]^2 + \frac{9}{16}B_0(B_0'-4)V_0\left[\left(\frac{V_0}{V}\right)^{2/3}-1\right]^3 \quad (2)$$

where E_0 - is the DFT ground state energy. B_0 – bulk modulus, B_0' - pressure derivative of the volumetric modulus (B'=(∂B/∂P)T), V-is the volume of the cell, V_0-equilibrium volume, that is, when the system is in a relaxing (ground) state.

The calculated optimized lattice parameters (a, b, c, and V) and bond lengths for all structures are shown in Table 1, and the experimental data are compared.

3. Results and Discussion

3.1. Structural properties.

Determination of the structural specification (optimized lattice constants (a, b,

Table 1. Comparison of calculated structural parameters with experimental ones.

$CsSnBr_{3-x}I_x$		**$CsSnBr_3$**	**$CsSnBr_2I$**	**$CsSnBrI_2$**	**$CsSnI_3$**
Lattice parameters, Å	This work	a = 8.3557 b = 11.730 c = 8.2055	a = 8.2064 b = 12.619 c = 8.2046	a = 8.4670 b = 12.551 c = 8.4675	a = 8.9081 b = 12.435 c = 8.4355
	Exp.	a= 8.3634 [13] b=11.760 [13] c=8.1782 [13]	-	-	a= 8.688 [14] b= 12.37 [14] c= 8.643 [14]
Volume, $Å^3$	This work	804.2926	849.6717	899.9003	934.4653
	Exp.	804.4168 [13]	-	-	929.4687 [14]

Comparison of the tabular data indicates that the calculated structural parameters for the unbiased systems $CsSnBr_3$ and $CsSnI_3$ are in good correlation with the experimental results (Table 1). However, there are no experimental data in the literature on comparing the lattice parameters of mixed perovskites $CsSnBr_2I$ and $CsSnBrI_2$.

Further, Figure 2 shows the dependences of the volume of nanocrystals of the $CsSnBr_{3-x}I_x$ ($0 \le x \le 3$) system on the iodine concentration.

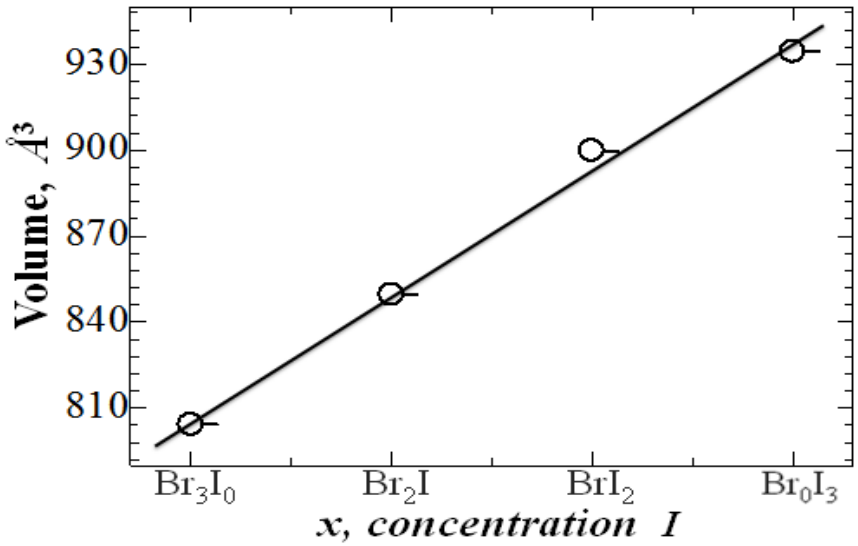

Figure 2. Change in the volume of the $CsSnBr_{3-x}I_x$ system depending on the Br/I ratio. Volume as a function of iodine concentration (x).

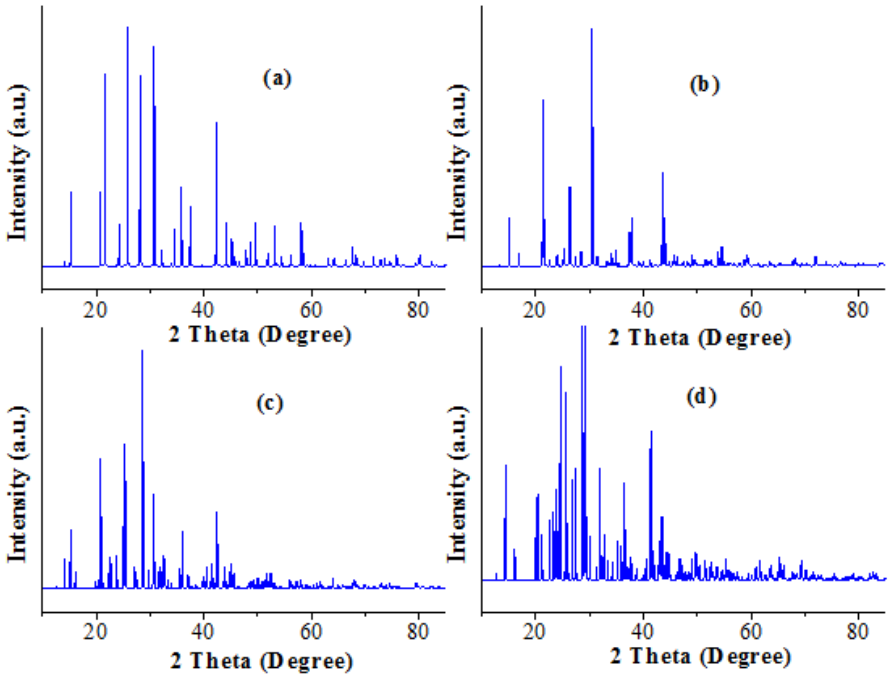

[14]. Yamada, K. Structural phase transitions of the polymorphs of $CsSnI_3$ by means of rietveld analysis of the X-ray diffraction. *Phys. Rev.A.* **1991**, *20*, 801-804, https://doi.org/10.1021/acs.inorgchem.0c00958.

[15]. Giorgio, S. Carbon Nanomaterials: Synthesis, Functionalization and Sensing Applications. *Nanomaterials* **2021**, *11,* 967, https://doi.org/10.3390/nano11040967.

[16]. Stanislav, Ch.; Xiaoliang, Q.; Kübler, Z. Tunable multifunctional topological insulators in ternary Heusler compounds. *Nature Materials* **2010**, *9*, 541-545, https://doi.org/10.1038/nmat2770.

[17]. Nematov, D. D.; Khusenzoda, M. A.; Burhonzoda, A.S.; Kholmurodov, Kh.T.; Lyubchyk, A.; Medhat I. Investigation of Structural and Optoelectronic Properties of N-Doped Hexagonal Phases of TiO_2 ($TiO_{2-x}N_x$) Nanoparticles with DFT Realization: OPTIMIZATION of the Band Gap and Optical Properties for Visible-Light Absorption and Photovoltaic Applications. *Biointerface research in applied chemistry* **2021**, *12*, 3836 – 3848, https://doi.org/10.33263/BRIAC123.3836 3848.

[18]. Nematov, D.D. Computer analysis of the electronic and structural properties of $CsSnI_3$:Cl and $CsPbI_3$:Cl nanocrystals [Нематов, Д. Компьютерный анализ электронных и структурных свойств нанокристаллов $CsSnI_3$:Cl и $CsPbI_3$:Cl]. *SCI-ARTICLE.RU* **2019**, *76*, 187-196, https://sci-article.ru/stat.php?i=1577288854.

[19]. Doroshkevich, A.; Nabiev, A.; et all. Frequency Modulation of the Raman Spectrum at The Interface DNA-ZrO_2 Nanoparticles. *Egyptian Journal of Chemistry* ***2019***, *62*, 13-20, https://doi.org/10.21608/ejchem.2019.12898.1806 .

[20]. Nematov, D.; Burkhonzoda, A.; Khusenov, M.; Kholmurodov, Kh.; Doroshkevich, A.; Doroshkevich, N.; Zelenyak, T.; Majumder, S. Molecular Dynamics of DNA Damage and Conformational Behavior on a Zirconium-Dioxide Surface. *Journal of Surface Investigation: X-ray, Synchrotron and Neutron Techniques* **2019**, *13*, 1165–1184, https://doi.org/10.1134/S1027451019060430.

[21]. Nematov, D.; Burkhonzoda, A.; Khusenov, M.; Kholmurodov, Kh.; Doroshkevich, A.; Doroshkevich, N.; Zelenyak, T.; Majumder, S; Ahmed, R.; Medhat, I. Molecular Dynamics Simulations of the DNA Radiation Damage and Conformation Behavior on a Zirconium Dioxide Surface. *Egyptian Journal of Chemistry* **2019**, *62*, 149-161, https://doi.org/10.21608/ejchem.2019.12981.1811.

[22]. Burkhonzoda, A; Giyosov, S.; Nematov, D.; Khusenov, M.; Kholmurodov, H. Quantum-mechanical calculation of the electronic structure of ZrO2:Ti^{4+} in the framework of the density functional theory. [Бурхонзода, А,; Гиёсов, С.; Нематов, Д.; Хусенов, М.; Холмуродов, Х. Кванто-механический расчет электронного строения ZrO_2:Ti^{4+} в рамках теории функционала плотности]. *Polytechnic Bulletin. Series: Intellect. Innovation. Investments [Политехнический вестник. Серия: Интеллект. Инновации. Инвестиции]* **2019**, *3*, 11-17.

[23]. Nematov, D.; Burhonzoda, A.; Khusenov, M.; Kholmurodov, Kh.; Yamamoto, T. First principles analysis of geometrical structure, electronic and optical properties of CsSnI3-xBrx perovskite for photoelectric applications. *Journal of Surface Investigation: X-ray, Synchrotron and Neutron Techniques* **2021**, *15*, 532–536, https://doi.org/10.1134/S1027451021030149.

[24]. Burkhonzoda, A.S.; Nematov, D.D.; Khodzhakhonov, I.T.; Boboshirov, D.I. Optical properties of nanocrystals of the $TiO_{2-x}N_x$ system [Оптические свойства нанокристаллов системы $TiO_{2-x}N_x$]. *SCI-ARTICLE.RU* **2021**, *92*, 176-187, https://sci-article.ru/stat.php?i=1621254426.

[25]. Burkhonzoda, A.S.; Nematov, D.D.; Kholmurodov, Kh.T. Structural and electronic properties of nanoscale thin films based on ZrO_2 [Структурные и электронные свойства наноразмерных тонких плекнок на основе ZrO2], *SCI-ARTICLE.RU* **2021**, *92*, 143-1152, https://sci-article.ru/stat.php?i=1623240070.

[26]. Nematov, D.D. Modeling the impact of ionizing radiation on the process of immobilization of biological molecules [Моделирование воздействия

ионизирующего излучения на процесс иммобилизации биологических молекул]. *SCI-ARTICLE.RU* **2020**, *81*, 12-35, https://core.ac.uk/download/344742895.pdf.

[27]. Nematov, D.D. MD modeling of the processes of interaction and encapsulation of nucleotides in the matrix of a carbon nanotube with gold nanoparticles [МД моделирование процессов взаимодействия и инкапсуляции нуклеотидов в матрице углеродной нанотрубки с наночастицами из золота]. *SCI-ARTICLE.RU* **2020**, *83*, 71-91, https://sci-article.ru/stat.php?i=1593585575.

[28]. Nematov, D.D. Research and optimization of optoelectronic properties of N-doped titanium dioxide ($TiO_{2-x}N_x$) nanoparticles for photovoltaic applications [Исследование и оптимизация оптоэлектронных свойств N-легированных наночастиц диоксида титана ($TiO_{2-x}N_x$) для фотоэлектрических применений]. *SCI-ARTICLE.RU* **2021**, *91*, 110-130, https://sci-article.ru/stat.php?i=1616187629.

[29]. Stephen, J. C.; John, D. D.; Josephine, A. H. Evidence for the direct population of solid-state bands by non-bonding electron pairs in compounds of the type $CsM_{II}X_3$(M_{II}= Ge, Sn, Pb; X = Cl, Br, I) . *J. Mater. Chem.* **1995**, *5*, 1813-1818, https://doi.org/10.1039/JM9950501813.

[30]. Zhuo, Ch.; Jian, J.; Wang, Y. Schottky solar cells based on $CsSnI_3$ thin-films/ *Appl. Phys. Lett.* **2012**, *101*, 093901, https://doi.org/10.1063/1.4748888.

[31]. Atchara, P.; Yongyut, L. Band alignment of cesium-based halide perovskites. *Ceram. Int.* **2018**, *44*, 161−163, https://doi.org/10.1016/j.ceramint.2018.08.124.

[32]. Stephen, J. C.; John, D. D. High-temperature Mössbauer studies on ^{119}Sn-enriched caesium tin(II) chlorides and bromides. *J. Chem. Soc., Dalton Trans.* **1995**, 2723-2727, https://doi.org/10.1039/DT9950002723.

[33]. Borriello, I.; Giovanni, C.; Domenico, N. Ab initio investigation of hybrid organic-inorganic perovskites based on tin halides. *Phys. Rev. B* **2008**, *77*, 235214, https://doi.org/10.1103/PhysRevB.77.235214.

[34]. Tripathy, A.; Behera, M.; Rout, A.S.; Biswal, S.K.; Phule, A.D. Optical, Structural, and Antimicrobial Study of Gold nanoparticles Synthesized Using an Aqueous Extract of Mimusops elengi Raw Fruits. *Biointerface Research in Applied Chemistry* **2021**, *10*, 7085-7096, https://doi:10.33263/briac106.70857096.

[35]. Najm, A.S.; Moria, H.; Ludin, N.A. Areca catechu as photovoltaic sensitizer for dye-sensitized solar cell (DSSC). *Biointerface Research in Applied Chemistry*, **2020**, *10*, 5636-5639, https://doi:10.33263/briac103.636639.

[36]. Mawloud, B.; Norredine, M.; Omar, A.; Aamir, H. Optoelectronic properties of the novel perovskite materials $LiPb(Cl:Br:I)^3$ for enhanced hydrogen production by visible photo-catalytic activity: Theoretical prediction based on empirical formulae and DFT. *International Journal of Hydrogen Energy* **2020**, *45,* 33466-33477, https://doi.org/10.1016/j.ijhydene.2020.09.066.

[37]. Christopher, J.; Christopher, J.; Jacob, M. Inorganic Halide Double Perovskites with Optoelectronic Properties Modulated by Sublattice Mixing. *J. Am. Chem. Soc.* **2021**, *142*, *11*, 5135–5145, https://doi.org/10.1021/jacs.9b12440.

[38]. Gleb, N. Z.; Larisa, A. M.; Tatyana, Y.P.; Larisa, A.S.; Elena, V. Simanina . Inhibition of Adenylate Cyclase of Regeneration-Competent Cells of Nervous Tissue: a Novel Approach for the Treatment of AlcoholicEncephalopathy. *Biointerface Research in Applied Chemistry* **2021**, *12,* 1547–1560, https://doi.org/10.33263/BRIAC122.15471560.

[39]. Maria, C.; Folgueras, M.; C, F.; Jianbo, J.; Mengyu, G.; Li, N. Q.; Julian, A. S.; Shivani, S.; Michael, B.; Ross, R. Z.; Fabian, S.; Kerstin, S-A.; Mark, A.; Peidong, Y Lattice Dynamics and Optoelectronic Properties of Vacancy-Ordered Double Perovskite Cs_2TeX_6 (X = Cl^-, Br^-, I^-) Single Crystals. *J. Phys. Chem. C* **2021**, *125*, 25126–25139, https://doi.org/10.1021/acs.jpcc.1c08332.

[40]. Husein, I.; Rahmawaty, V.; Kinarya, E.; Patonah, N. The effect of photoconductive mole fraction based on thin film $Ba_xSr_{1-x}TiO_3$ (X=0.000; 0.125; 0.250; 0.375; 0.500) on electrical properties and diffusivity coefficient. *Biointerface Research in Applied*

Chemistry, **2021**, *11*, 14956-14963, https://doi.org/10.33263/BRIAC116.1495614963.

[41]. Jingjing, L.; Junle, Q.; Thomas, K.; Jun, S. Optoelectronic devices based on the integration of halide perovskites with silicon-based *materials. J. Mater. Chem. A* **2021**, *9,* 20919-20940, https://doi.org/10.1039/D1TA04527J.

[42]. Bhanu, M.; Venkata, S.; Sriram, M.; Hussen, M.; Syam, S.; Basavaiah, Ch. Photocatalytic Activity of Heavy Metal Doped CdS Nanoparticles Synthesized by Using Ocimum sanctum Leaf Extract. *Biointerface Research in Applied Chemistry* **2021**, *11*, 12547 - 12559, https://doi.org/10.33263/BRIAC115.1254712559.

[43]. Nematov, D. D.; Burhonzoda, A. S.; Khusenov, M. A.; Kholmurodov, K. T.; Ibrahim, M. A. The quantum-chemistry calculations of electronic structure of boron nitride nanocrystals with density Functional theory realization. *Egyptian Journal of Chemistry* **2019**, *62*, 21-27, doi:10.21608/EJCHEM.2019.12879.1805.

[44]. Xiang, G.; Wu, Y.; Li, Y.; Cheng, C.; Leng, J.; Ma, H. Structural and Optoelectronic Properties of Two-Dimensional Ruddlesden–Popper Hybrid Perovskite $CsSnBr_3$. *Nanomaterials*, **2021,** *11*(8), 2119, doi:10.3390/nano11082119.

[45]. Zhang, F.; Ma, Z.; Shi, Z.; Chen, X.; Wu, D.; Li, X.; Shan, C. Recent advances and opportunities of lead-free perovskite nanocrystal for optoelectronic application. *Energy Material Advances* **2021**, *5198145*, doi.org/10.34133/2021/5198145.